Author for correspondence:
Haytam Kasem
e-mail: mehaytam@technion.ac.il

Royal Society Publishing
Informing the science of the future

Effect of counterface roughness on adhesion of mushroom-shaped microstructure

Haytam Kasem and Michael Varenberg

Department of Mechanical Engineering, Technion, Haifa 32000, Israel

In this study, the effect of the substrate roughness on adhesion of mushroom-shaped microstructure was experimentally investigated. To do so, 12 substrates having different isotropic roughness were prepared from the same material by replicating topography of different surfaces. The pull-off forces generated by mushroom-shaped microstructure in contact with the tested substrates were measured and compared with the pull-off forces generated by a smooth reference. It was found that classical roughness parameters, such as average roughness (R_a) and others, cannot be used to explain topography-related variation in pull-off force. This has led us to the development of an integrated roughness parameter capable of explaining results of pull-off measurements. Using this parameter, we have also found that there is a critical roughness, above which neither smooth nor microstructured surface could generate any attachment force, which may have important implications on design of both adhesive and anti-adhesive surfaces.

1. Introduction

The problem of quick and easy reversible attachment is of great importance in different fields of technology. For this reason, inspired by high-performance attachment systems of some lizards, spiders and insects allowing them to adhere and run on inverted surfaces [1], a new field of adhesion science has emerged during the past decade. Several works [2–5] focused on understanding the physics behind the spectacular performance of these systems have confirmed that the structural and functional principles used by biological systems may be utilized to design artificial surfaces with enhanced adhesion capacity. In the light of this finding, many attempts have been made to amplify adhesion of a flat contact by modifying contact geometry, which opened a race for new bioinspired dry adhesives [6–10] (and many more, for recent review see reference [11]).

One of a few truly working dry biomimetic adhesives developed so far is the one based on mushroom-shaped contact elements [12]. Inspired by the adhesive hairs evolved in male beetles from the family Chrysomelidae, this type of attachment system performs well on smooth substrates, while being able to generate strong pull-off force nearly without any preload. The potential of this artificial attachment system has been verified in allowing a 120 g walking robot to climb smooth vertical surfaces [13] and, very recently, a 70 kg person to hang on a glass ceiling [14].

Much research has been carried out on studying various properties of mushroom-shaped adhesive microstructure and the effects of preload and contamination [12], shear [15], overload [16], tilt [17], hierarchy [18], ambient pressure [19], oil lubrication [20] and submerging underwater [21] were elucidated. Following experimental research, theoretical explanations of mushroom shape advantages were also provided [22,23]. However, the effect of counterface roughness on adhesion of biomimetic mushroom-shaped microstructure has not been systematically studied yet. It is obvious that the counterface roughness is a vital factor that may affect the design of microstructured adhesives [20]. For this reason, in this study, we investigate the effect of roughness and identify the key roughness parameters responsible for the observed variation in pull-off force.
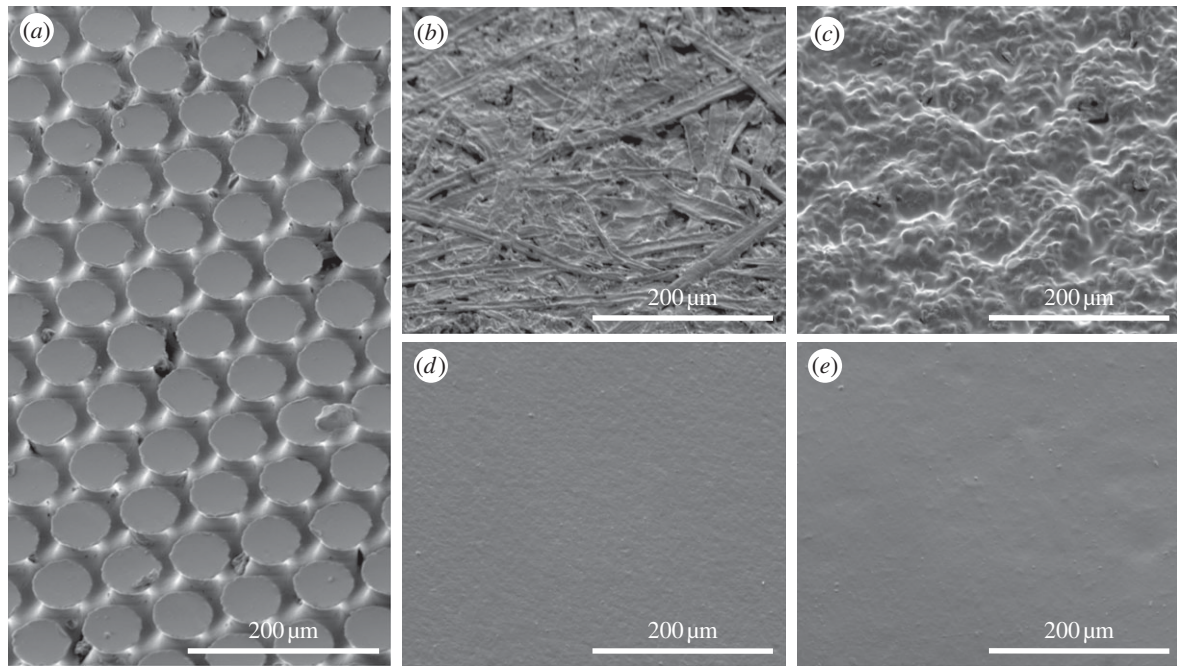
Figure 1. Mushroom-shaped adhesive microstructure made of (*a*) PVS and Epoxy counterfaces (*b*) 6, (*c*) 4, (*d*) 1, (*e*) 5, with numbers according to table 1.

Table 1. Mean roughness parameters measured at three different sites on each Epoxy replica.

replica	R_a (µm)	R_{max} (µm)	R_{pk} (µm)	S_m (mm)	σ_s (µm)	β (µm)	η (µm^{-2})	original surface
1	0.193	0.306	0.306	0.048	2.010	24.554	0.045	abrasive paper
2	0.953	1.070	1.070	0.054	4.718	11.253	0.005	abrasive paper
3	1.683	1.587	1.587	0.075	4.137	9.473	0.004	abrasive paper
4	2.287	2.253	2.253	0.075	5.390	7.651	0.003	abrasive paper
5	0.237	0.393	0.393	0.064	4.472	24.439	0.037	microscope slide
6	2.510	2.087	2.087	0.103	2.956	8.058	0.003	office paper
7	1.767	2.173	2.173	0.090	4.426	12.414	0.004	hard paper
8	1.010	0.520	0.520	0.160	8.712	19.859	0.007	hard paper
9	1.793	0.897	0.897	0.358	9.728	20.953	0.011	microscope base
10	4.363	2.807	2.807	0.339	10.327	15.212	0.008	office table
11	1.230	0.927	0.927	0.169	3.818	19.871	0.008	hard paper
12	2.270	1.383	1.383	0.440	7.619	20.977	0.013	plastic folder

2. Material and methods

2.1. Specimen

Mushroom-shaped microstructure (figure 1*a*) was manufactured [24] by Gottlieb binder GmbH (Holzgerlingen, Germany) at room temperature by pouring two-compound polymerizing poly(vinyl-siloxane) (PVS; Coltène Whaledent AG, Altsätten, Switzerland) into the holed template lying on a smooth support. After polymerization, the ready-to-use cast tape of about 0.3 mm in width with Young's modulus of about 3 MPa [25] was removed from the template. Mushroom-shaped microstructure consisted of hexagonally packed pillars of about 100 µm in height bearing terminal contact plates of about 50 µm in diameter (figure 1*a*). The area density of the terminal contact plates was about 48%. The backside of the cast microstructured tape was used for smooth reference surface. To prepare the samples, the tape was placed on a glass support while facing either structured or smooth side up. Then, the same

two-compound fast-polymerizing PVS was poured onto this tape from above. Prospective specimen height was defined by the spacers placed between the support and a covering flat surface that was used to squeeze superfluous polymer out of the gap. Using disposable biopsy Uni-Punch (Premier Products Co., Plymouth Meeting, PA, USA), samples of 2 mm in diameter were punched out of the resulting 1 mm height PVS casts having either structured or smooth contact surface and always smooth back surface. To fix the samples, we glued their smooth back surface to the specimen holders using the same PVS.

Counterface samples of $15 \times 4 \times 1$ mm^3 in size replicating 12 surfaces of different isotropic roughness (figure 1*b*–*d* and table 1) were cast out of 2 Ton Clear Weld Epoxy, (ITW Devcon, Riviera Beach, FL, USA) using a two-step moulding technique [26]. This helped studying the effect of surface topography only, while avoiding introduction of material-related differences in adhesion. The surfaces to be replicated were
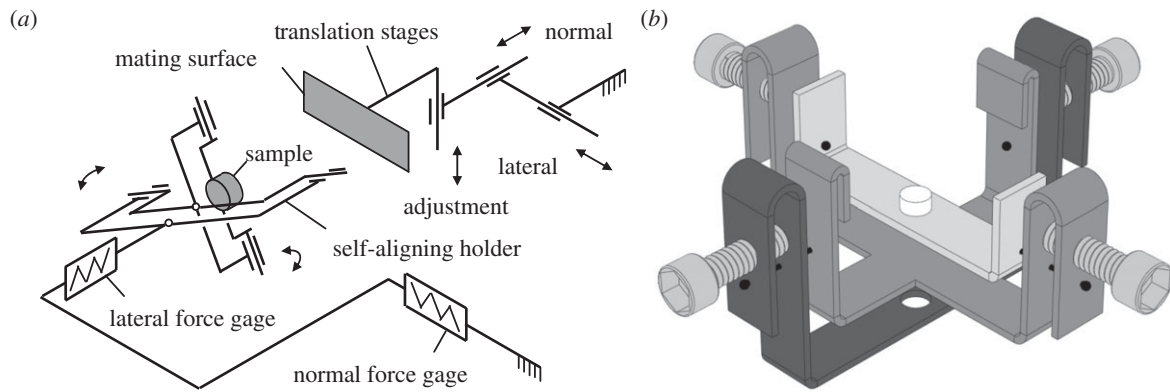
Figure 2. (a) Schematic of the home-made tribometer used [27]. (b) Passive self-aligning sample holder based on two orthogonal axes of rotation coplanar with the contact plane [27]. The system is made much more user-friendly by using thread-tightening screws simplifying considerably preliminary adjustments.

chosen from various office and laboratory objects, such as table, folder, different types of paper, microscope base and microscope slide, so to cover as large a range of roughness as possible.

2.2. Equipment

Surface appearance of the specimens used was imaged in an FEI Quanta 200 environmental scanning electron microscope (FEI Co., Brno, Czech Republic). Surface roughness was measured with a mechanical profiler Hommel LV-100 (Hommelwerke GmbH, Villingen-Schwenningen, Germany). The tests were performed on a home-made tribometer [27] incorporating two main units used for driving and measuring purposes (figure 2a). The drive unit consists of three motorized translation stages used to load the contact by moving the mating surface. The measurement unit consists of two load cells used to determine the forces acting on the sample. To guarantee full contact and fulfil the 'equal load sharing' principle [28] during pull-off force measurements in a flat-on-flat contact scheme, essential in surface texture testing, a passive self-aligning system of specimen holders was used (figure 2b).

2.3. Procedure

Each test started by bringing the Epoxy counterface in contact with the PVS sample. Taking into account that pull-off force generated in flat-on-flat contact is independent of the preload [12], only one normal load was applied in this study. After applying the normal load of 90 mN (nominal contact pressure of about 29 kPa), the pull-off force was measured while withdrawing the translation stage at a velocity of 100 μm s^{-1}. Each tribo-pair was tested at least five times, each time on a different region of the counterface. Prior to experiments, the samples were washed with deionized water and liquid soap, and then dried in blowing nitrogen. The experiments were carried out at temperature and relative humidity of 20–22°C and 55–60%, respectively.

3. Results and discussion

Average values of pull-off force measured between the PVS specimens and the Epoxy counterfaces are reported in table 2. Simple comparison of the obtained results shows that at certain types of roughness mushroom-shaped microstructure adheres more than 40 times stronger than smooth surface made of the same material, whereas, in other cases, both types of specimens generate the same negligible adhesion. Obviously, this results from the differences in topography of counterfaces leading to different contact conditions (figure 3). In order to better understand the relationship between surface texture and

Table 2. Mean values of pull-off force measured between the PVS specimens and the Epoxy counterfaces.

replica	structured surface pull-off force, P_s (mN)	smooth surface pull-off force, P_f (mN)	P_s/P_f
1	217.3	33.6	6.47
2	5.7	0	n.a.
3	1.2	0	n.a.
4	0	0	n.a.
5	185.0	48.4	3.82
6	0	0	n.a.
7	16.2	0.8	19.29
8	112.2	8.9	12.54
9	162.1	14.7	11.00
10	107.0	2.4	44.58
11	170.7	23.5	7.26
12	208.0	7.6	27.37

operation, we have analysed results of the measured pull-off force as a function of various roughness parameters. Figure 4 presents the pull-off force generated by mushroom-shaped microstructure and smooth surface as a function of the counterface R_a. It is clear that there is no correlation between the pull-off force and the R_a, as nearly the same force can be achieved on the surfaces characterized by the R_a values differing by approximately an order of magnitude, and vice versa. In addition to R_a, we have also tested the effect of other classical roughness parameters, such as maximum roughness depth R_{max}, reduced peak height R_{pk}, mean spacing of profile irregularities S_m, etc. (table 1), and obtained the same lack of correlation between any single parameter and the measured pull-off force.

Taking into account the fact that the only difference between the adhesion of tested counterfaces comes from the variation in their roughness (all other parameters are kept constant), it is reasonable to assume that there is a certain roughness characteristic capable of correlating with the observed changes in pull-off force. Analysing the surface features that may affect adhesion, it is possible to come to the conclusion that the most important role is played by the surface asperities [29]. It is obvious that the more asperities
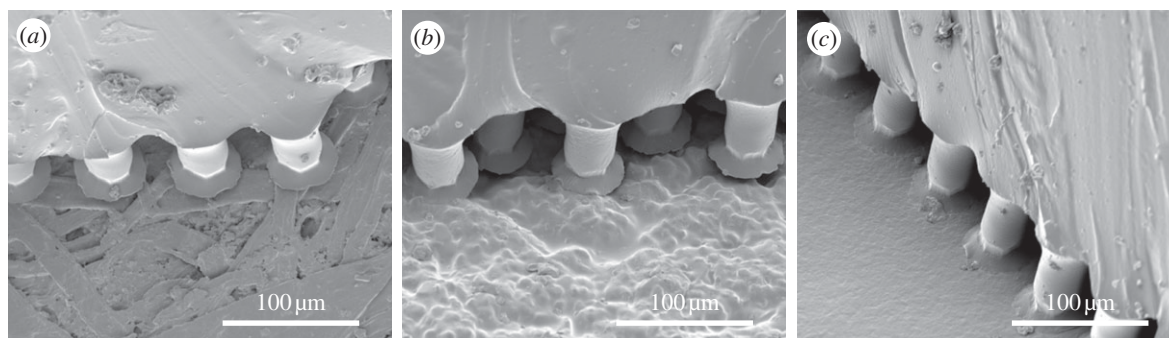
Figure 3. Mushroom-shaped adhesive microstructure in contact with Epoxy counterfaces (*a*) 6, (*b*) 4 and (*c*) 1, with numbers according to table 1.
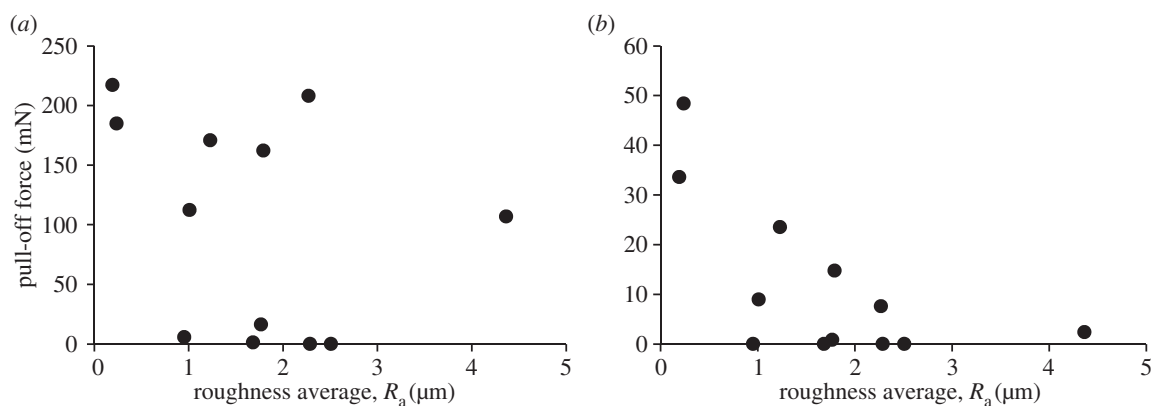

Figure 4. (*a*) Pull-off force of mushroom-shaped PVS microstructure and (*b*) smooth PVS surface presented as a function of the Epoxy counterface roughness average R_a.

(contact points) the surface bears, the larger the adhesion is. Similarly, asperities of larger radius generate larger adhesion [30,31]. On the other hand, adhesion decreases with increasing dispersion of asperity heights [29]. Based on these tendencies and using the surface density of asperities η, the mean radius of asperity summits β and the standard deviation of asperity height distribution σ_s [32], we defined a new adhesion-oriented integrative roughness parameter R_i:

$$R_i = \frac{\sigma_s}{\beta\eta}.$$

Parameters σ_s, β and η are not readily calculated by standard roughness analysis software, so we have obtained them using the following approach [33,34]. First, each digitized profilometric trace (we have measured three traces for each substrate) was analysed to determine spectral moments m_0, m_2, m_4

$$m_0 = \text{AVG}[(z^2)],$$
$$m_2 = \text{AVG}\left[\left(\frac{dz}{dx}\right)^2\right],$$
$$m_4 = \text{AVG}\left[\left(\frac{d^2z}{dx^2}\right)^2\right],$$

where the AVG operator computes the arithmetic average, and $z(x)$ is the surface height profile. Then, assuming isotropic roughness of a normally distributed height, the values of σ_s, β and η were obtained from the spectral moments of each digitized trace as

$$\sigma_s = \left(m_0 - 0.8968\frac{m_2^2}{m_4}\right)^{1/2},$$

$$\beta = 0.375\left(\frac{\pi}{m_4}\right)^{1/2},$$

$$\eta = \frac{m_4}{6\pi\sqrt{3}m_2}.$$

Finally, to compute the R_i for each substrate, the values of σ_s, β and η were averaged (table 1) for three corresponding traces.

Figure 5 presents the pull-off force generated by mushroom-shaped microstructure and smooth surface as a function of a new roughness parameter R_i. This chart shows a clear correlation between the two in both microstructured and smooth samples. The effect of roughness, however, is different in two types of surfaces. In smooth surface, the pull-off force decreases with increasing roughness of counterface with approximately constant rate, whereas in microstructured surface, the pull-off force first decreases slowly, remaining on nearly the same level across a wide range of roughness, and then falls sharply at certain critical roughness. This means that mushroom-shaped microstructure is much more robust and tolerant to irregularities of the counterface, resulting in a more than 40-fold increase in pull-off force that may be achieved in comparison with smooth surface made of the same material.

Yet another interesting point is that, surprisingly, the critical roughness at which the pull-off force approaches zero is the same despite entirely different topography of both types of the tested elastomeric samples. This may possibly mean that each pair of materials has its own critical roughness characterizing the passage from an adhesive to a non-adhesive surface state. This concept may find wide use in designing surfaces of tailored adhesive properties. The question of whether this assumption is true, however, remains open and calls for further research.
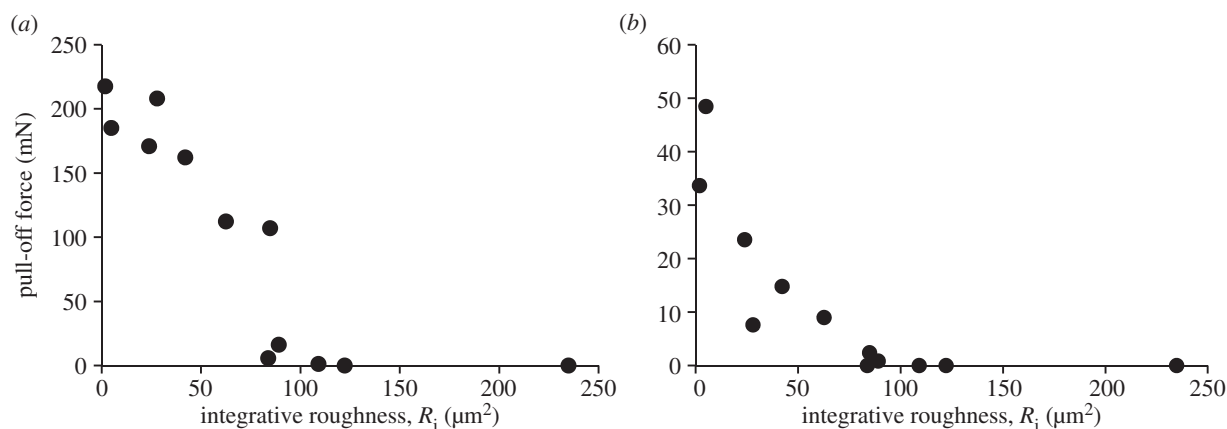
Figure 5. (*a*) Pull-off force of mushroom-shaped PVS microstructure and (*b*) smooth PVS surface presented as a function of the Epoxy counterface integrative roughness R_i.

4. Conclusion

The measurements performed demonstrate that attachment ability of mushroom-shaped microstructure is less sensitive to a variation in counterface roughness than smooth surface made of the same material. This robustness supplements a list of advantages that this texture has in possession and gives more weight to the reasons why many naturally evolved biological attachment systems are based on mushroom-shaped geometry [35].

Analysing the effects of roughness, we have shown that classical parameters cannot be used to explain topography-related variation in pull-off force. This has led us to the development of an R_i capable of presenting the pull-off force data in a readable way. Using this parameter, we have also found that there is a critical roughness, above which neither smooth nor microstructured surface can generate any adhesion. This newly developed parameter may have important implications on design of both adhesive and anti-adhesive surfaces.

References

1. Scherge M, Gorb SN. 2001 *Biological micro- and nanotribology: nature's solutions*. Berlin, Germany: Springer.

2. Persson BNJ. 2003 On the mechanism of adhesion in biological systems. *J. Chem. Phys.* **118**, 7614–7621. (doi:10.1063/1.1562192)

3. Glassmaker NJ, Jagota A, Hui CY, Kim J. 2004 Design of biomimetic fibrillar interfaces. I. Making contact. *J. R. Soc. Interface* **1**, 23–33. (doi:10.1098/rsif. 2004.0004)

4. Tian Y, Pesika N, Zeng H, Rosenberg K, Zhao B, McGuiggan P, Autumn K, Israelachvili J. 2006 Adhesion and friction in gecko toe attachment and detachment. *Proc. Natl Acad. Sci. USA* **103**, 19 320–19 325. (doi:10.1073/pnas.0608841103)

5. Varenberg M, Pugno N, Gorb S. 2010 Spatulate structures in biological fibrillar adhesion. *Soft Matter* **6**, 3269–3272. (doi:10.1039/c003207g)

6. Geim AK, Dubonos SV, Grigorieva IV, Novoselov KS, Zhukov AA, Shapoval SY. 2003 Microfabricated adhesive mimicking gecko foot-hair. *Nat. Mater.* **2**, 461–463. (doi:10.1038/nmat917)

7. Kim S, Sitti M. 2006 Biologically inspired polymer microfibers with spatulate tips as repeatable fibrillar adhesives. *Appl. Phys. Lett.* **89**, 261911. (doi:10. 1063/1.2424442)

8. Greiner C, del Campo A, Arzt E. 2007 Adhesion of bioinspired micropatterned surfaces: Effects of pillar radius, aspect ratio, and preload. *Langmuir* **23**, 3495–3502. (doi:10.1021/la0633987)

9. Glassmaker NJ, Jagota A, Hui CY, Noderer WL, Chaudhury MK. 2007 Biologically inspired crack trapping for enhanced adhesion. *Proc. Natl Acad. Sci. USA* **104**, 10 786–10 791. (doi:10.1073/pnas. 0703762104)

10. Parness A, Soto D, Esparza N, Gravish N, Wilkinson M, Autumn K, Cutkosky M. 2009 A microfabricated wedge-shaped adhesive array displaying gecko-like dynamic adhesion, directionality and long lifetime. *J. R. Soc. Interface* **6**, 1223–1232. (doi:10.1098/rsif. 2009.0048)

11. Jagota A, Hui CY. 2011 Adhesion, friction, and compliance of bio-mimetic and bio-inspired structured interfaces. *Mat. Sci. Eng. R* **72**, 253–292. (doi:10.1016/j.mser.2011.08.001)

12. Gorb S, Varenberg M, Peressadko A, Tuma J. 2007 Biomimetic mushroom-shaped fibrillar adhesive micro-structure. *J. R. Soc. Interface* **4**, 271–275. (doi:10.1098/rsif.2006.0164)

13. Daltorio KA, Gorb S, Peressadko A, Horchler AD, Ritzmann RE, Quinn RD. 2005 A robot that climbs walls using micro-structured polymer feet. In *Proc. Int. Conf. Climbing and Walking Robots*, London, UK, pp. 131–138.

14. Heepe L, Kovalev AE, Varenberg M, Tuma J, Gorb SN. 2012 First mushroom-shaped adhesive microstructure: a review. *Theor. Appl. Mech. Lett.* **2**, 014008. (doi:10.1063/2.1201408)

15. Varenberg M, Gorb SN. 2007 Shearing of fibrillar adhesive microstructure: friction and shear-related changes in pull-off force. *J. R. Soc. Interface* **4**, 721–725. (doi:10.1098/rsif.2007.0222)

16. Varenberg M, Gorb S. 2008 Close-up of mushroom-shaped fibrillar adhesive microstructure: contact element behavior. *J. R. Soc. Interface* **5**, 785–789. (doi:10.1098/rsif.2007.1201)

17. Murphy MP, Aksak B, Sitti M. 2009 Gecko-inspired directional and controllable adhesion. *Small* **5**, 170–175. (doi:10.1002/smll.200801161)

18. Murphy MP, Kim S, Sitti M. 2009 Enhanced adhesion by gecko-inspired hierarchical fibrillar adhesives. *Appl. Mater. Interfaces* **1**, 849–855. (doi:10.1021/am8002439)

19. Heepe L, Varenberg M, Itovich Y, Gorb SN. 2011 Suction component in adhesion of mushroom-shaped microstructure. *J. R. Soc. Interface* **8**, 585–589. (doi:10.1098/rsif.2010.0420)

20. Kovalev A, Varenberg M, Gorb S. 2012 Wet versus dry adhesion of biomimetic mushroom-shaped microstructure. *Soft Matter* **8**, 3560–3566. (doi:10. 1039/c2sm25431j)

21. Varenberg M, Gorb S. 2008 A beetle-inspired solution for underwater adhesion. *J. R. Soc. Interface* **5**, 383–385. (doi:10.1098/rsif.2007.1171)

22. Spuskanyuk AV, McMeeking RM, Deshpande VS, Arzt E. 2008 The effect of shape on the adhesion of fibrillar surfaces. *Acta Biomater.* **4**, 1669–1676. (doi:10.1016/j.actbio.2008.05.026)

23. Carbone G, Pierro E, Gorb SN. 2011 Origin of the superior adhesive performance of mushroom-shaped microstructured surfaces. *Soft Matter* **7**, 5545–5552. (doi:10.1039/c0sm01482f)

24. Tuma J. 2007 Process for creating adhesion elements on a substrate material. US Patent 20070063375 A1.

25. Peressadko A, Gorb SN. 2004 When less is more: experimental evidence for tenacity enhancement by division of contact area. *J. Adhes.* **80**, 247–261. (doi:10.1080/00218460490430199)

26. Gorb SN. 2007 Visualization of native surfaces by two-step molding. *Microsc. Today* **15**, 44–47.

27. Murarash B, Varenberg M. 2011 Tribometer for in situ scanning electron microscopy of microstructured contacts. *Tribol. Lett.* **41**, 319–323. (doi:10.1007/s11249-010-9717-y)

28. Hui CY, Glassmaker NJ, Tang T, Jagota A. 2004 Design of biomimetic fibrillar interfaces: 2. Mechanics of enhanced adhesion. *J. R. Soc. Interface* **1**, 35–48. (doi:10.1098/rsif.2004.0005)

29. Fuller KNG, Tabor D. 1975 The effect of surface roughness on the adhesion of elastic solids. *Proc. R. Soc. Lond. A* **345**, 327–342. (doi:10.1098/rspa.1975.0138)

30. Johnson KL, Kendall K, Roberts AD. 1971 Surface energy and the contact of elastic solids. *Proc. R. Soc. Lond. A* **324**, 301–313. (doi:10.1098/rspa.1971.0141)

31. Derjaguin BV, Muller VM, Toporov YP. 1975 Effect of contact deformations on the adhesion of particles. *J. Colloid Interface Sci.* **53**, 314–326. (doi:10.1016/0021-9797(75)90018-1)

32. Greenwood JA, Williamson JBP. 1966 Contact of nominally flat surfaces. *Proc. R. Soc. Lond. A* **295**, 300–319. (doi:10.1098/rspa.1966.0242)

33. McCool JI. 1987 Relating profile instrument measurements to the functional performance of rough surfaces. *ASME J. Tribol.* **109**, 264–270. (doi:10.1115/1.3261349)

34. Pawar G, Pawlus P, Etsion I, Raeymaekers B. 2013 The effect of determining topography parameters on analyzing elastic contact between isotropic rough surfaces. *ASME J. Tribol.* **135**, 011401. (doi:10.1115/1.4007760)

35. Gorb SN, Varenberg M. 2007 Mushroom-shaped geometry of contact elements in biological adhesive systems. *J. Adhes. Sci. Technol.* **21**, 1175–1183. (doi:10.1163/156856107782328317)